

## Surface morphology of active layers for VCSEL application

W.Strupinski<sup>1)</sup>, M.Wesolowski<sup>1)</sup>, A.Jasik<sup>1)</sup>

1) III–V Epitaxy Dept., Institute of Electronic Materials Technology, ul. Wolczynska 133, 01–919 Warsaw, Poland

Commonly provided technique for VCSEL fabrication of 1.55 and 1.31  $\mu\text{m}$  emission is the wafer bonding. Applying InGaAsP/InP active layer and AlGaAs/GaAs Bragg mirrors high quality vertical cavity surface emitting lasers can be produced. Metal substrate bonding is the method used also for fabrication of InGaAs/GaAs strained VCSELs 980nm emission. This technique is also possible to apply for InGaAsP/GaAs 808nm lasers. The surface morphology of active layers and mirrors is the most important factor for consideration in the case of this structures production method. The Aixtron 200 MOCVD reactor was employed to produce InGaAsP/InP, InGaAs/GaAs and InGaAsP/GaAs active layers.

We have tested the InGaAsP/InP active layer structures for 1.31  $\mu\text{m}$  VCSELs. Structures were InGaAsP/InP  $1/2\lambda$  and  $3/2\lambda$  cavities. Bottom and top layers of these structures were composed by  $\text{In}_{0.85}\text{Ga}_{0.15}\text{As}_{0.38}\text{P}_{0.62}$  lattice matched to InP material with energy gap corresponding to 1.1  $\mu\text{m}$ .

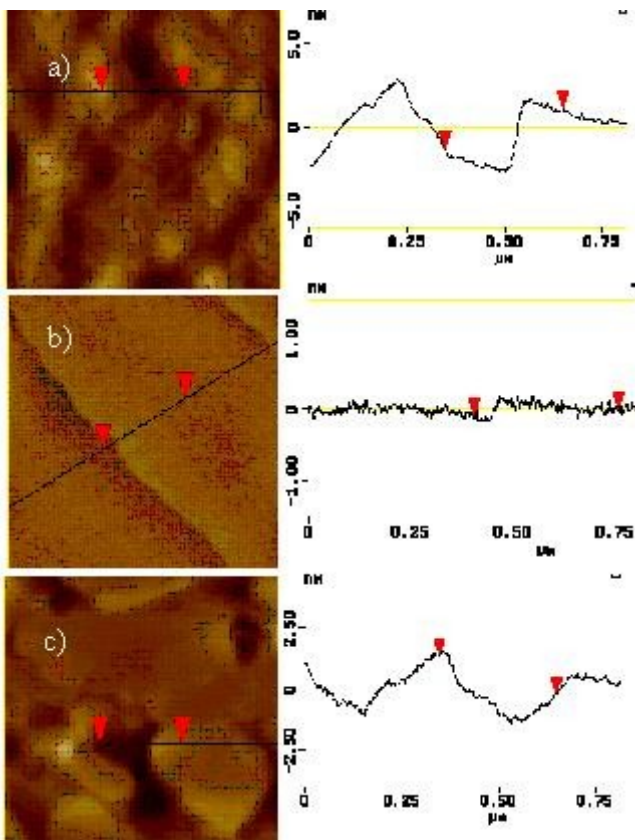


**Fig.1.** AFM images of InGaAsP/InP  $\lambda=1.1\mu\text{m}$  surfaces when sample cooled in: a)  $\text{AsH}_3 + \text{PH}_3$  atmosphere, b)  $\text{PH}_3$  atmosphere, c) when kept for 20min in  $\text{AsH}_3 + \text{PH}_3$  atmosphere, then cooled in  $\text{PH}_3$  atmosphere.

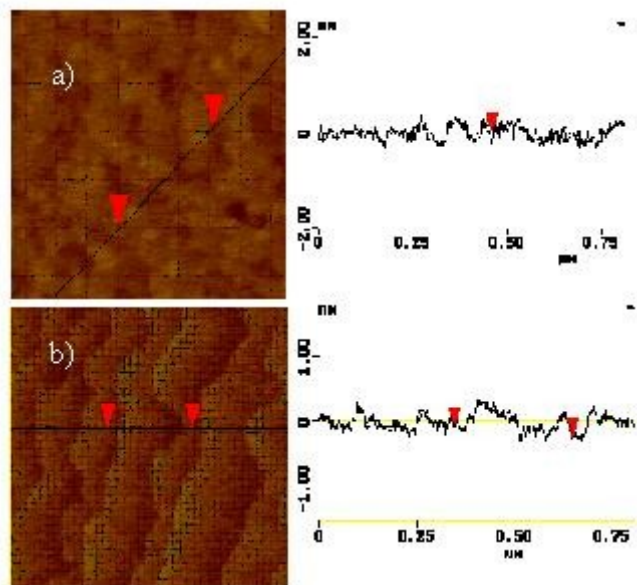


**Fig.2.** AFM images of InGaAsP/InP  $\lambda=1.3\mu\text{m}$  surfaces when sample cooled in: a)  $\text{AsH}_3 + \text{PH}_3$  atmosphere, b)  $\text{PH}_3$  atmosphere.

The structure was designed to provide wafer bonding technique by applying AlGaAs/GaAs Bragg reflectors. Upper reflectors were directly bonded to as-grown InGaAsP surface. Typical growth was pursued at reactor pressure of 100mbars and temperature of 655°C. Resolved by x-ray diffractometry lattice mismatch to InP was on the level of 300ppm. The natural idea of structure final cooling in the reactor is the usage of gas atmosphere composed by group V carriers as during the growth of the last top layer. Resulting surface observed by AFM is presented in the Fig.1a, exhibiting a few nm deep fractures that principally disables further direct wafer bonding. To recognize causes of such behavior we tested a few modifications of initial process. Processes indicated the crucial role of the cooling atmosphere. When sample was cooled in PH<sub>3</sub> with the absence of AsH<sub>3</sub> the surface was ideal with visible single atomic terraces as shown in Fig.1b. To exclude the influence of temperature on the equilibrium AsH<sub>3</sub>/PH<sub>3</sub> ratio, we left the surface for 20min in the reactor after the growth of the last layer in the AsH<sub>3</sub>/PH<sub>3</sub> ratio and temperature as during the growth. The surface as shown in Fig.1c was similar to initial one with deep fracture. Such results indicated, the surface reconstruction occurs when InGaAsP is exposed for a few minutes after closing group III flows, even in the atmosphere (behind group III) and temperature optimized for the growth. Presence of the AsH<sub>3</sub> in cooling atmosphere leads to dissolution of the surface. In both InGaAsP/InP VCSEL structures proper growth conditions and adequate cooling led to ideal surfaces and if the flatness resulted from the substrate quality and the reactor flows geometry is satisfying, wafer bonding do not exhibit any serious problems. The dissolution effect is dependent on the InGaAsP composition. When tested for In<sub>0.72</sub>Ga<sub>0.28</sub>As<sub>0.61</sub>P<sub>0.39</sub> lattice matched to InP with energy gap corresponding to 1.3μm, dissolution affected the surface much lower. The AFM image shown in Fig.2a represents a sample cooled with the PH<sub>3</sub>/AsH<sub>3</sub> ratio the same as during the growth.

The InGaAsP/GaAs material in opposite to InGaAsP/InP one meets technological difficulties, however VCSEL structures based on InGaAsP/GaAs are designed and metal-wafer bonding technique can be applied to obtain efficient, highly thermal conductive Bragg reflectors. Typical 808nm laser structure consists InGaP lattice matched to GaAs cladding layers, In<sub>1-x</sub>Ga<sub>x</sub>As<sub>y</sub>P<sub>1-y</sub>/GaAs ( $\lambda=695\text{nm}$ ,  $x \cong 0.30$ ,  $y \cong 0.15$ ) barriers and In<sub>0.09</sub>Ga<sub>0.91</sub>As<sub>0.82</sub>P<sub>0.18</sub>/GaAs QW ( $\lambda=821\text{nm}$ ). There are two effects complicating growth of structures composed with InGaAsP/GaAs: vicinity of the miscibility gap during the MOCVD growth [1] and the ordering effect [2] in the sense of sequential growth of InAsP/GaAsP layers in [1,1,5] direction. First effect occurs for arsenic content  $y$  in In<sub>1-x</sub>Ga<sub>x</sub>As<sub>y</sub>P<sub>1-y</sub> between 0.2 and 0.4 for 700°C temperature, the second effect occurs when  $y$  is close to 0 (InGaP and  $y < 0.1$ ). Both effects seem to disturb not only optical and lattice properties of the layer, but also its surface. Structures are also higher sensitive on the lattice mismatch than it is in case of InGaAsP/InP. We have grown active 808nm laser layers and examined surfaces. The problem with morphology was best seen in case of low arsenic InGaAsP ( $\lambda=695\text{nm}$ ,  $y=0.15$ ) and in case of thick  $\sim 1\mu\text{m}$  – InGaP.

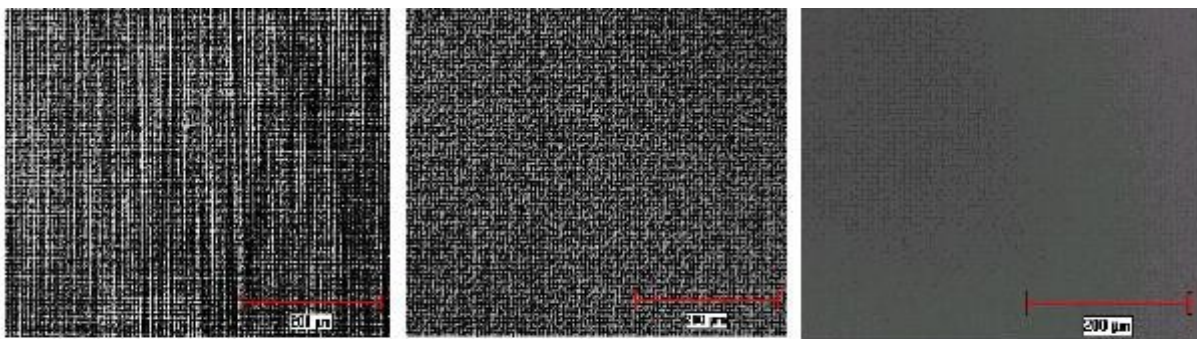


**Fig 3.** Nomarsky photographs of InGaP/GaAs surfaces: a) thickness  $d=0.8\mu\text{m}$ , lattice mismatch  $\Delta a/a=+2400\text{ppm}$ , growth rate  $r=1.5\mu\text{m/h}$ , b)  $d=0.8\mu\text{m}$ ,  $\Delta a/a\approx 0\text{ppm}$ ,  $r=1.5\mu\text{m/h}$ , c)  $d=1.5\mu\text{m}$ ,  $\Delta a/a\approx 0\text{ppm}$ ,  $r=4.5\mu\text{m/h}$ .

There are reported data indicating improvement of such layers properties by increasing V/III ratio and the growth temperature, but our tests indicated strongest influence of the growth rate (Fig.3). High growth rate above 4  $\mu\text{m/h}$  produced good surface, when low growth rate exhibited clearly seen under Nomarsky microscope growth nonuniformity – as shown in Fig.3b. Also optical properties of such layers very strongly improved after the increase of the growth rate.

InGaAs/GaAs strained VCSEL structures were also dedicated for wafer bonding technology, thus ideal smooth epi-layer surface was isolated as a key parameter. In order to achieve the required emission of 980 nm the indium content was calculated as 20%. The value of theoretical critical thickness for such composition was well above the applied InGaAs strained layers, however careful optimisation of InGaAs growth was performed using PL, Nomarsky contrast and AFM tools. It was found that the combination of high growth temperature and low growth rate resulted in the smooth surface with the roughness within 1 ML (Fig.4).

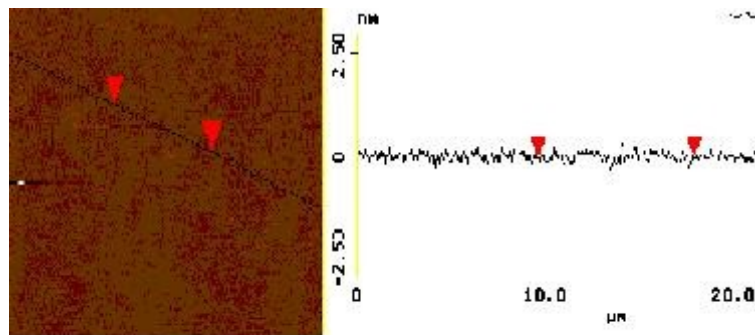


Fig.4 AFM image of InGaAs/GaAs 4 QWs.

Kinetic thermal activated processes on the wafer surface and low group III mass transport towards substrate allowed to achieve the lowest roughness. PL spectrum was very narrow (19nm at FWHM) and stable between growth runs.

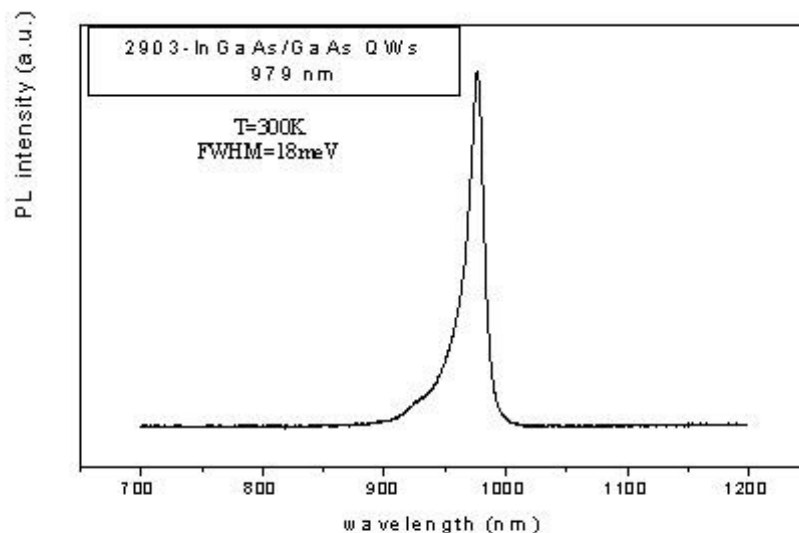


Fig.5. PL spectrum of InGaAs/GaAs 4 QWs heterostructure.

The growth rate was optimized by diminishing of gallium mass transport by factor 4 in comparison to the deposition of GaAs layer. The reactor pressure was kept at 100 mbar and TMGa source at 0°C. The earlier attempts of growth in lower temperature did not give better surface, however PL intensity was stronger but unstable between processes and within 2-inch wafer. Interruption of the growth did not succeed in surface improvement, either. VCSEL structure contained 4 InGaAs wells 8 nm of thickness and GaAs barriers. Keeping optimized parameters of the growth IML surface roughness of the whole heterostructure could be achieved repeatedly.

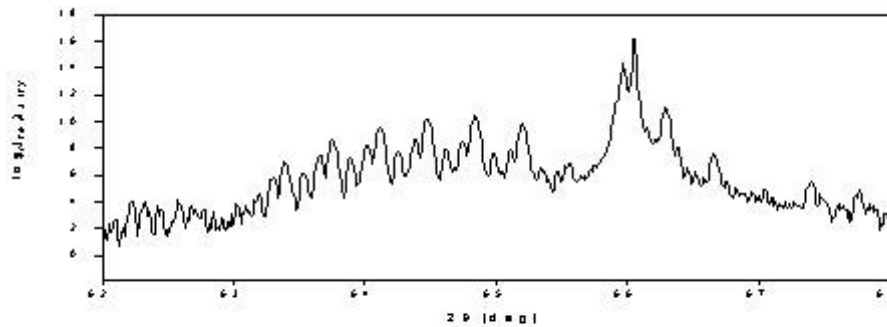


Fig.6. X-ray measurements results of VCSEL heterostructure.

X-ray studies confirmed ideality of interfaces and structural quality (Fig.6).

#### Literature.

- [1] M. Kondow, H. Kakibayashi, S. Minagawa, J. Crystal Growth 88 (1988) 291–296.
- [2] K. Onabe, Jpn. J. Of Applied Phys. 21, 797 (1982).